Predictive modelling of compressive strength in silicon nitride-reinforced aluminium composites using supervised machine learning: a comparative study of random forest and artificial neural networks

K. Venkateswara Reddy[1*], *Suresh* Gudala[2], *Rajasekhar* Thota[3], *Lava* Kumar *P*[4], *Dhiraj* Raj[5], *Ramesh* Ganugapenta [6]

[1]SR University, Warangal, Telangana, 506371, India
[2]Senior Scientist, Serbian Institute of science and technology, Russia
[3]Mohan Babu University, School of Engineering, Tirupati, Andhra Pradesh, India
[4]Department of Mechanical Engineering,CVR College of Engineering, Vastunagar, Hyderabad, India
[5]Shivalik college of Engineering, Department of Mechanical, Dehradun, Uttarakhand, India
[6]Vemu Institute of Technology, Dept. Of Mechanical, Andhra Pradesh, India

Abstract. The integration of machine learning and material science is now changing the way property predictions are made, accelerating the process of discovery and optimization of advanced materials. For this research, we employed a supervised ML to estimate the compressive strength of AMCs reinforced by silicon nitride. To sharpen predictive accuracy, hyperparameter tuning using GridSearch CV was performed. We employed two different algorithms-RF and ANN-to unravel the complex links between the inputs, such as compaction pressure, reinforcement content, sintering temperature, and sintering time with the target strength. Regularization was used to guard against overfitting, and training versus testing performance was compared rigorously. The results indicated that the RF outperformed the ANN model, giving an R^2 of 0.88, while the ANN reached an R^2 of only 0.80. These results suggested that the RF model had tighter residuals and higher accuracy since it emphasizes the parameters that drive most of the variance in the dataset. This work illustrates the potential of ML, especially RF, in reliably predicting properties of materials and informing the design of high-performance composites.

1 Introduction

Among the modern approaches to mechanical property prediction, such as compression and hardness of aluminum composites, supervised ML proved to be one of the most powerful. Combined with experimental data, these algorithms provide researchers with actionable knowledge for the optimization of target composition and processing parameters toward desired performance. The following section represents a summary of some recent studies,

[*]Corresponding author: venkatmpie@gmail.com

selection of algorithms, and take-home messages [1]. Many ML techniques have predicted the mechanical properties of aluminum composites with success. ANN is one of the popular approaches because it models the nonlinear relationship between inputs and outputs. ANN has been developed to predict the green density, sintered density, and hardness of Al-Al2O3 MMCs as a function of volume fraction, compact pressure, and milling time. ANN was thus able to capture the interaction between reinforcement content and heat treatment conditions in predicting hardness of LM4 based composites reinforced with TiB_2.

Mechanical properties of aluminium composites were successfully predicted by several machine learning algorithms. ANNs have been widely used because of their capabilities in modelling the complex relationship between input parameters and output properties. ANN models, as an instance, have been used to predict green density, sintered density, and hardness of Al-Al2O3 MMCs by considering volume fraction, compact pressure, and milling time [2]. Hardness of multistage solutionized and artificially aged LM4 + TiB2 composites was predicted by ANN with high accuracy of modeling reinforcement content-heat treatment condition interactions [3].

Deep learning models have been extended to predict the microhardness and ultimate tensile strength in coconut shell particle-reinforced aluminum matrix composites through models such as CPPNN. These depend on data regarding fractions of CSP, conditions of casting, and mechanical tests for the prediction of new formulations with high accuracy [4]. These models are trained on datasets comprising CSP fraction values, compo-casting conditions, and mechanical test results, thus allowing for accurate predictions of new composite formulations.

Other promising approaches include RF, GB, and SVR. For example, RF was used to predict yield and tensile strength of aluminum alloys from their chemical composition, with R^2 values for the former property in excess of 0.9. Another example is the use of a Sequential Minimal Optimization SVR variant for predicting tensile strength and hardness in Cu–AA7075 nanocomposites, which gave the best correlation among several different models tested. The present paper is intended to develop and compare RF and ANN models for the prediction of compressive strength in silicon nitride-reinforced aluminum composites. We tune these models with GridSearch CV to optimize hyperparameters and improve accuracy. We also seek to identify which independent features-Compaction Pressure, Reinforcement Composition, Sintering Temperature, and Sintering Time-most strongly influence compressive strength.

The study will contrast RF and ANN by considering accuracy, R^2, and residuals, while regularization will be included in order to avoid overfitting and support generalizability [5]. Further, feature importance analysis will be performed to understand how ANN selects parameters that contribute to a majority of the data variance [6]. Overall, this work demonstrates the transformative potential of ML, particularly ANN, in the accurate prediction of material properties and their insights into the design, optimization, and development of high-performance composites.

The present paper therefore aims at developing and comparing RF and ANN supervised machine learning models for the prediction of compressive strength of silicon nitride-reinforced aluminium composites. The research will fine-tune these models using GridSearch CV techniques for optimization of hyperparameters with the aim of improving predictive accuracy. Furthermore, it looks to find from among the independent features-Compaction Pressure, Reinforcement Composition, Sintering Temperature, and Sintering Time-the main ones that greatly influence the Compressive Strength of the composites. This work has compared RF and ANN model performances based on accuracy, R^2, and residual distribution, aside from including techniques for regularization to prevent overfitting and ensure model generalizability. Feature importance analysis to understand how the ANN model gives priority to parameters that contribute to a majority of the variance in the dataset has also been conducted. This work tries to demonstrate the transformational role of machine learning, especially ANN, in the prediction of material property with good accuracy and provide valuable insight into the design, optimization, and development of high-performance composites.

2 Materials and methods

The study focused on the AA7075/SiN composite, with AA7075 as the matrix material and Silicon Nitride as the reinforcement. The mechanical behavior of the composite was explored in terms of its compression strength, varying the conditions of processing. The major input parameters involved in the present study included SiN composition, compaction pressure, sintering temperature, and sintering time. Experimental trials yielded 172 data points that formed the dataset for training and testing machine learning models. In developing predictive models, Artificial Neural Networks and Random Forest were implemented to establish accurate relationships between input parameters and compression strength. GridSearchCV was used to perform the tuning of hyperparameters with a view to extracting better results from the models. The model performance was assessed based on R^2 scores, regression plots, and residual analysis [7].

3 Results and discussions

3.1 Machine learning model evaluation

3.1.1 Visualization of data and mechanical properties analysis

Figure 1: Pairplot analysis that offers insight into the interactions of several processing parameters on the mechanical properties of the composite. It can be seen that SiN Composition and Compression Strength are positively correlated, proving that mechanical properties increase with reinforcement content. Similarly, Sintering Temperature and Compression Strength are on a positive trend, showing that higher sintering temperatures result in densification and proper bonding between matrix and reinforcement. Also, the relation between SiN Composition and Sintering Temperature further confirms that with increasing reinforcements, higher sintering temperatures are needed to allow for diffusion bonding [8]. On the other hand, the Compaction Pressure vs Sintering Time scatter plot does not reveal any outstanding relation, clearly indicating that compaction pressure has negligible effects on sintering time. Also, SiN Composition vs Compression Strength shows some degree of scatter because at higher concentrations of reinforcement, agglomeration may occur, which restricts effective load transfer. Also, there is no trend observed for the Sintering Time vs Compression Strength plot, indicating that longer sintering does not appreciably improve the mechanical properties and leads to grain growth [9]. Histograms along the diagonal of the pairplot provide information on the distribution of individual parameters. Accordingly, fairly uniform distributions were represented for SiN Composition, Compression Strength, and Sintering Temperature, whereas Compaction Pressure and Sintering Time had distinct peaks, indicating that experimental conditions had been more frequently used.

Figure 2, above, is the Pearson correlation heatmap representing relationships in quantitative terms with regard to the processing parameters. A high positive correlation of 0.97 between SiN Composition and Sintering Temperature indicates that reinforcement content directly influences the sintering conditions: higher temperatures are required for effective diffusion bonding. The correlation of 0.67 between SiN Composition and Compression Strength validates that with an increase in reinforcement content, strength increases. On the other hand, a moderate correlation value of 0.70 between Compaction Pressure and Compression Strength itself indicates that while higher compaction pressure helps to a great extent in densification, it is not the major or leading factor affecting strength [10]. The Sintering Temperature-Compression Strength has a correlation of 0.62, which signifies that higher temperatures help toward densification, decreasing porosity, thus improving strength. However, the Sintering Time-Compression Strength correlation is fairly low, at 0.29, indicating further improvement in strength may not be possible by prolonging the sintering time; rather, it will lead to grain coarsening itself [11].

In general, dataset trends indicate that the most influential parameters governing the mechanical behavior of the composite are SiN Composition, Sintering Temperature, and Compression Strength. The strong reinforcement content-sintering temperature correlation underlines the need to optimize sintering conditions in order to enhance densification and interfacial bonding. On the other hand, Compaction Pressure shows a moderate contribution to Compression Strength; thus, compared to the rest of the processing parameters, it is in a secondary position. Furthermore, the weak influence of Sintering Time on Compression Strength shows that too long a sintering duration is not necessary and might result in detrimental microstructural changes such as grain coarsening. The present findings point out the need to balance reinforcement levels, sintering conditions, and compaction pressure in order to achieve an optimum in the mechanical properties of the composite.

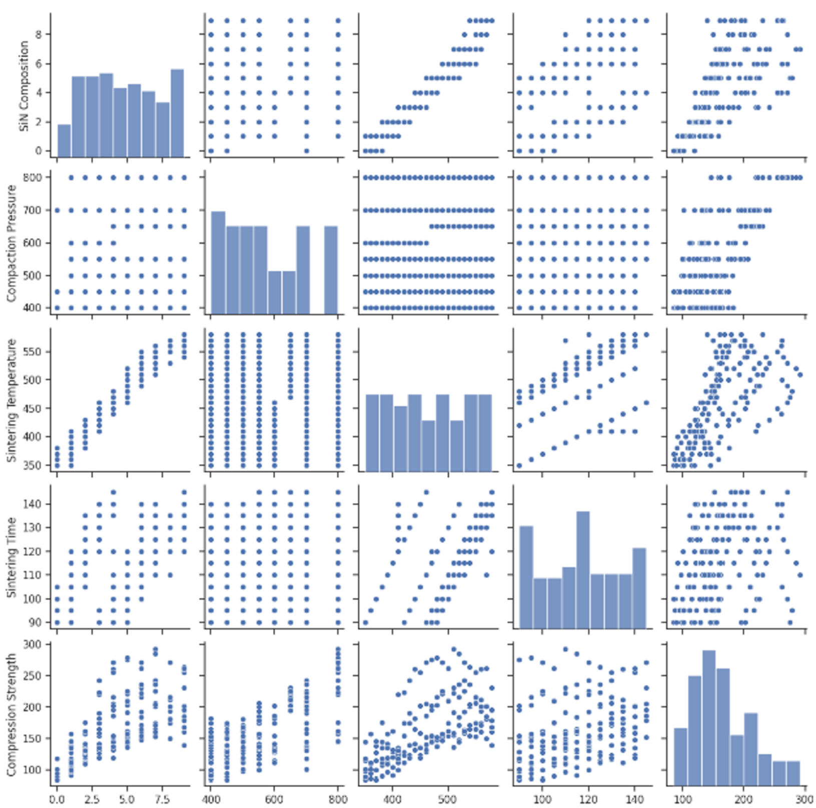

Fig. 1. Pairplot and heatmap of the data used in the present work.

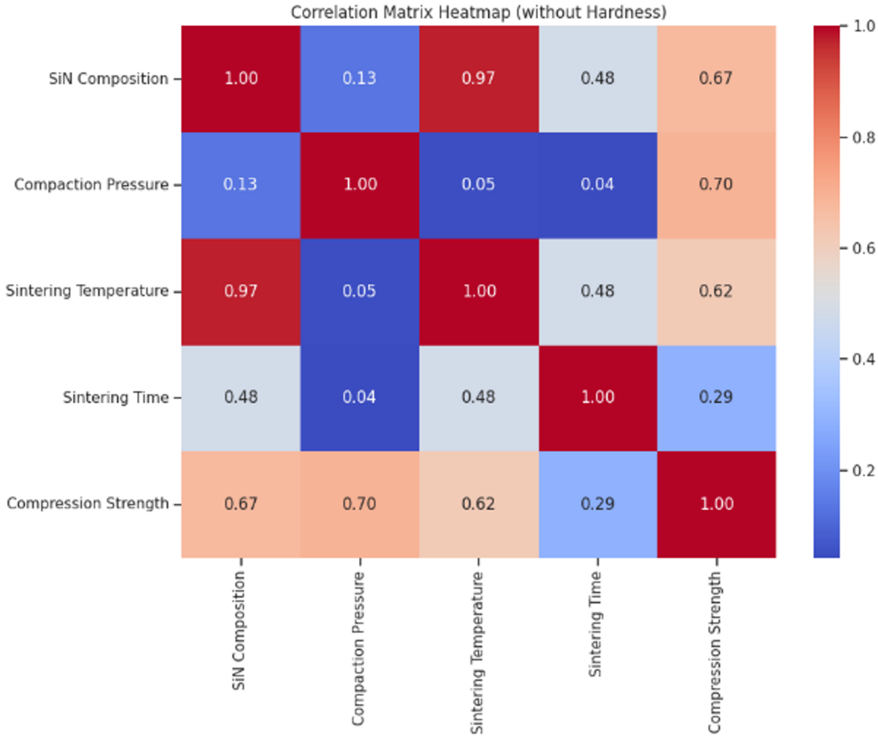

Fig. 2. Heatmap between the process parameters and outputs in the present work.

3.1.2 Machine learning models evaluation

The bar chart Figure 3 compares the training and testing R^2 scores of Artificial Neural Networks (ANN) and Random Forest (RF) models, with hyperparameters optimized using GridSearchCV. The Random Forest model achieved higher performance, with an R^2 score of 0.92 for training and 0.88 for testing, indicating strong generalization and minimal overfitting. In contrast, the ANN model obtained an R^2 score of 0.85 for training and 0.80 for testing, showing relatively lower predictive accuracy compared to RF. The optimized RF model (max_depth=10, min_samples_leaf=1, min_samples_split=2, n_estimators=200) demonstrated a better fit, as evident from its higher R^2 values. The slight difference between the training and testing scores suggests that the model generalizes well without significant overfitting. The ANN model (activation=relu, alpha=0.0001, hidden_layer_sizes=(50,50), solver=adam), while also achieving a reasonable fit, showed a more noticeable drop between training and testing scores, which may indicate that the neural network requires further tuning, such as adjusting the number of hidden layers, neurons, or regularization strength, to enhance generalization. The optimized hyperparameters are listed in Table 1. Overall, Random Forest outperforms ANN in this study, achieving better predictive accuracy and robustness, likely due to its ability to handle complex relationships and non-linearity effectively. However, ANN could still be improved by fine-tuning hyperparameters, increasing training data, or modifying network architecture to enhance performance further.

Table 1. Optimized hyperparameters obtained through gridsearchCV technique.

Random Forest	Artificial Neural Network
max_depth': 10 min_samples_leaf': 1 min_samples_split': 2 n_estimators': 200	activation: 'relu' 'alpha': 0.0001 hidden_layer_sizes': (50, 50) solver: 'adam

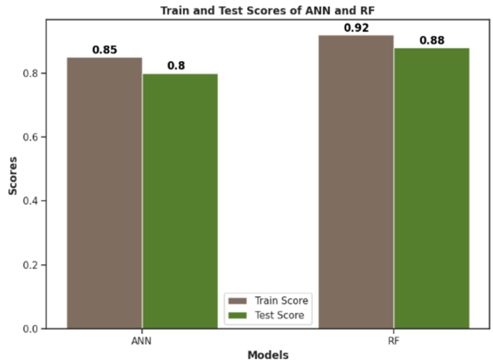

Fig. 3. R square values while training and testing for ANN and RF models.

3.1.2.1 Random forest (RF)

The actual versus predicted values for the Random Forest model is shown visually by the regression curve in Figure 4, which shows the performance of the model. The blue scatter points show the predicted values against the actual values, and the red dashed line is the ideal line of perfect prediction where all points would fall if the predictions exactly matched the actual values. Most of the points line up on this line, so the Random Forest model appears to have achieved a high level of accuracy in predicting the target variable. However, some scatter can be seen, especially at higher actual values, indicating minor deviations in the prediction [12]. For the obtained R^2 score from the Random Forest model, an R^2 score of 0.88 was realized on the test set, meaning that 88% of the variance in the actual values is explained by the model. This large R^2 value suggests a good predictive capability, which further corroborates the slight clustering of points around the perfect prediction line. At the same time, however, minor deviations at higher values indicate the model might slightly underpredict or overpredict at extreme ends. Because the train score of 0.92 was only a little higher than the test score of 0.88, there is minimal overfitting since the generalization capability remains strong.

Figure 5 shows the residual analysis, which helps determine the model errors and biases. The left plot, Residuals Spread - RF, shows the residuals, which are the differences between the actual and predicted values, versus the predicted values. For a well-fitted model, residuals are expected to be scattered in a random manner around zero, with no discernible pattern. In this plot, most of the residuals are equally placed around the zero line; thus, the model does not seem to have high bias. However, a few points with higher residual values indicate that the predictions do have some amount of variance, especially for higher actual values [13]. The right plot, Residual Histogram with Normal Curve - RF, depicts more of the residual distribution. The histogram indicates that residuals are approximately symmetric around zero, but slightly skewed, confirming that while most predictions are good, some are outliers. The superimposed normal curve, depicted by the red line, helps in assessing the normality of residuals. Near normality of residuals suggests that the model's errors are random, without systematic bias, which further confirmation for the validity of the model's predictions.

The observations from Figures 4 and 5 align well with the obtained R^2 score of 0.88 on the test set. The high value of R^2 is further supported by the strong alignment of predicted values with actual values in the regression plot, hence indicating that this model captures the underlying relationship in data quite well. Moreover, random dispersion of residuals and an approximate normal distribution of errors show that this model is well-calibrated without significant overfitting. Although the small gap between training and testing scores - 0.92 and 0.88, respectively - indicates that this model generalizes well, some minor deviations in residuals at higher predicted values do point to potential improvements. Fine-tuning of hyperparameters like max_depth or n_estimators, or a range of feature engineering techniques, would further reduce the variance in the predictions [14].

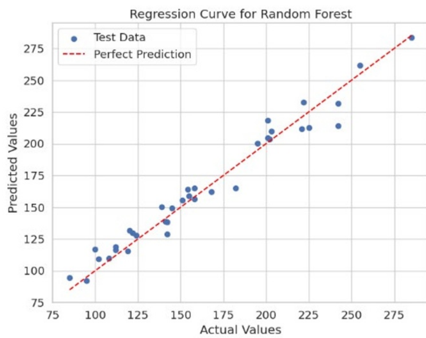

Fig. 4. Regression curve for RF model.

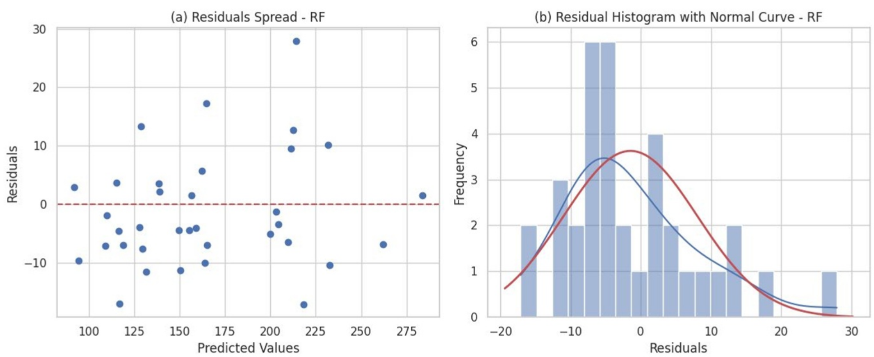

Fig. 5. Residual analysis for RF models.

3.1.2.2 Artificial neural network (ANN)

The regression curve for the Artificial Neural Network (ANN) model, shown in Figure 6, provides a visual representation of how well the model predicts the actual values. The blue scatter points represent the predicted values against the actual values, while the red dashed line denotes the ideal perfect prediction line where predictions match the actual values exactly. A well-performing model should have most of its predictions closely aligned along this red line. However, compared to the Random Forest model, the ANN regression plot shows a greater amount of scatter, indicating a reduced predictive accuracy. The R^2 score of ANN on the test set is 0.80, suggesting that 80% of the variance in the actual values is captured by the model, while 20% remains unexplained. This is lower than the 0.88 R^2 score of the RF model, indicating that the ANN model has relatively poorer generalization capability.

Another key observation from the regression plot is that several predictions are significantly deviating from the perfect prediction line, which especially occurs for higher actual values. This would hint that ANN is struggling more in predicting extreme values, which might be due to a limited number of hidden layers or neurons unable to capture the complex non-linearity in the dataset. Moreover, ANN models require extensive tuning and training to give optimum results, and in this case, further hyperparameter optimization was needed, such as increasing the number of hidden layers, adjusting the learning rate, or using different activation functions. Figure 7, showing the residual analysis, sheds more light on the prediction errors of the ANN model. The left plot, Residuals Spread - ANN, depicts the distribution of residuals, or better said, the differences between actual and predicted values, across the predicted values. A well-calibrated model should have residuals that randomly scatter around zero and do not show any pattern. The right plot, Residual Histogram with Normal Curve - ANN, further emphasizes the residual distribution. The blue bars represent the frequency of residuals, while the red normal curve shows the idealized distribution. Residuals seem more spread out and less centered around zero than in the RF model, indicating that prediction errors happen more often and are larger in size.

3.1.3 Comparative analysis of ML models

Figure 3 presents the bar chart comparing two models, Artificial Neural Networks and Random Forest, both of which had their hyperparameters optimized using GridSearchCV. Random Forest is on top, with an R^2 of 0.92 in training and 0.88 in testing, signaling a good generalization and little overfitting. On the other hand, ANN performed a bit worse, with an R^2 of 0.85 in training and 0.80 in testing, indicating its lower predictive accuracy compared to RF. The best RF setup (max_depth=10, min_samples_leaf=1, min_samples_split=2, n_estimators=200) has fitted the data well, as evidenced by its higher R^2 values. The narrow gap between the training and testing scores suggests a nice generalization of the model without notable overfitting. In the case of ANN (activation=relu, alpha=0.0001, hidden_layer_sizes=(50,50), solver=adam), the fitting is reasonable but the drop from training to testing is more pronounced. This might hint that further tuning-for instance, changing the number of layers or neurons, or even adjusting regularization-can lead to better generalization. The optimized hyperparameters are summarized in Table 1. On the whole, RF outperforms ANN in this study, giving better predictive accuracy and robustness, because it works better on complicated relations and nonlinearity. However, ANN may still be improved by careful hyperparameter tuning, more training data, or architectural changes that can push its performance further [15].

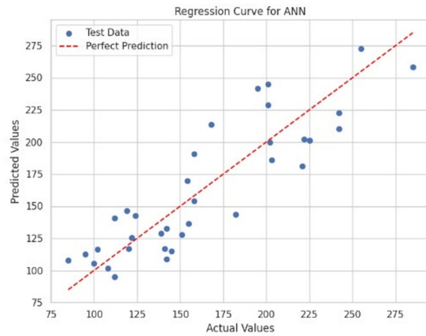

Fig. 6. Regression curve for ANN model.

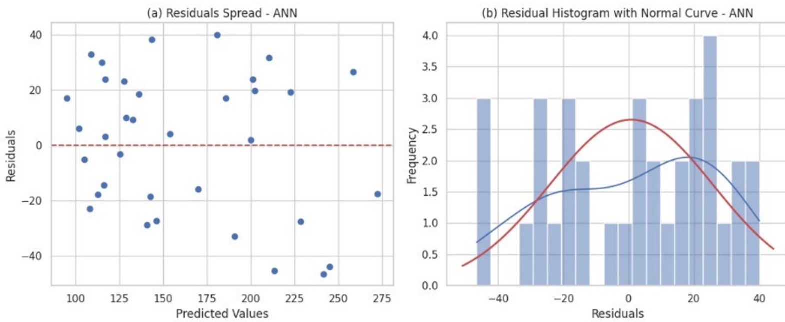

Fig. 7. Residual analysis for ANN model.

4 Conclusions

- RF outperforms ANN in predictive accuracy, with R^2 0.88 vs. 0.80, besides better generalization and smaller residuals.
- RF predictions are also in reasonably good agreement with the actual values, and the residuals show little scatter, whereas the ANN shows more scatter with a greater residual spread.
- ANN is showing promise but needs further optimization, such as tuning hidden layers, regularization, and training strategies, to improve accuracy and reduce variability.
- The findings confirm that RF is effective in capturing the complex patterns in material behavior, thus being more reliable in predicting mechanical properties. Given further refinement, ANN could also achieve a similar level of reliability.
- ANN requires extensive tuning, thereby increasing computational cost and training time, particularly for smaller and medium-sized data sets.
- By contrast, RF performs well with modest tuning and thus is more viable when data are limited but both accuracy and efficiency are needed.

References

1. N. Yilmaz, E. Baltaci, O. Baygin, T. Tüzüner, S. Ozkaya, A. Canakci, Effect of the usage of Er,Cr:YSGG laser with and without different remineralization agents on the enamel erosion of primary teeth, Lasers Med Sci 35 (2020) 1607–1620. https://doi.org/10.1007/s10103-020-03015-0.

2. A. Kumar, M.V.N.V. Satyanarayana, P.R. Mattli, A. Bhowmik, Enhanced Performance of AA7075/SiC/ZrC Hybrid Composite through Microwave Assisted Powder Metallurgy Techniques, J Mater Eng Perform 34 (2025) 4336–4349. https://doi.org/10.1007/s11665-024-09405-7.
3. K.V. Reddy, C.R. Reddy, Microstructural, mechanical and damping analysis of Al/Gr composites produced via friction stir processing: effect of rotational speed, Canadian Metallurgical Quarterly (2025) 1–10. https://doi.org/10.1080/00084433.2025.2508105.
4. K. Venkateswara Reddy, Dynamic mechanical and microstructural analysis of graphite-reinforced Al6061 alloy processed by friction stir processing, J Adhes Sci Technol (2025) 1–11. https://doi.org/10.1080/01694243.2025.2508752.
5. S. Thapliyal, R. Mamedipaka, Investigating the performance of aluminium-steel bimetallic structure fabricated through Wire and Arc Additive Manufacturing with interlayer approach, Structures 72 (2025). https://doi.org/10.1016/j.istruc.2025.108304.
6. H. Yu, Q. Zhao, J. Fu, Y. Hu, J. Liang, J. Li, W. Xu, The design of oxidation resistant Ni superalloys for additive manufacturing, Addit Manuf 97 (2025) 104616. https://doi.org/10.1016/j.addma.2024.104616.
7. V.S.S. Venkatesh, P.R. Vundavilli, M.M. Mahapatra, A. Goyal, A. Bhowmik, Extraction of kaolin and tribo informative analysis of the Al-kaolin composite through machine learning approaches, Sci Rep 15 (2025) 13370. https://doi.org/10.1038/s41598-025-97782-x.
8. K. Liu, L. Zhang, L. Cao, T. Wang, J. Fu, J. Wang, J. Zhang, X. Yang, Y. Cao, B. Liu, X. Li, Y. Gan, Binder jetting additive manufacturing of a 95W-3.5Ni-1.5Fe tungsten heavy alloy: Enhanced ductility and dynamic deformation mechanisms, Materials Science and Engineering: A 942 (2025) 148719. https://doi.org/10.1016/j.msea.2025.148719.
9. A. Kumar, Exploring the Effects of Ball Milling and Microwave Sintering on Microstructural and Mechanical Behavior of AA7075/SiC/ZrO2 Hybrid Composites, Silicon (2024). https://doi.org/10.1007/s12633-024-02856-6.
10. M.V.N.V. Satyanarayana, S.R. Maity, K.M. Pandey, V. Reddy, B. Pasha Mahammod, Effect of fabrication techniques on mechanical and microstructural behavior of AA7075/SiC/ZrC hybrid composite, Ceram Int 49 (2023) 37782–37792. https://doi.org/10.1016/j.ceramint.2023.09.106.
11. M.V.N. V Satyanarayana, V.K.S. Jain, K.K. Kumar, A. Kumar, S. Sundar, Influence of Cooling Media on the Electrochemical Behavior of Friction Stir Processed Al2014 Alloy, JOM 75 (2023) 526–536. https://doi.org/10.1007/s11837-022-05611-7.
12. Vaishali, From fabrication to prediction: unraveling the tensile strength of Al/SiN composites through machine learning, International Journal on Interactive Design and Manufacturing (IJIDeM) (2025). https://doi.org/10.1007/s12008-025-02274-x.
13. G. Manohar, Machine learning approaches for tensile strength prediction in Al/B4C metal matrix composites: a comparative analysis of neural networks and ensemble methods, International Journal on Interactive Design and Manufacturing (IJIDeM) (2025). https://doi.org/10.1007/s12008-025-02347-x.
14. R. Kumar, P. Mastanaiah, A. Kumar, Microstructural Characterization and Mechanical Properties of Wire and Arc Additively Manufactured 18% Ni Maraging Steel 250, J Mater Eng Perform (2025). https://doi.org/10.1007/s11665-025-12339-3.
15. A. Bhowmik, A.J. Santhosh, Predictive Modelling of Tensile Strength and Hardness of Microwave Assisted AA7075/Sic Composite Through Supervised Machine Learning

Algorithms, Results in Engineering (2025) 107793.
https://doi.org/10.1016/j.rineng.2025.107793.